Cutoff Rates of Multichannel MFSK and DPSK Signals in Mobile Satellite Communications

Yu T. Su, *Member, IEEE,* and Ju-Ya Chen

***Abstract*— This paper studies the coded performance of multichannel MFSK and DPSK signalings in mobile satellite environments characterized by various kinds of multipath fading. Rician, Rician/lognormal, and a convex combination of Rician and Rician/lognormal or Rayleigh/lognormal distributions are used to model these communication channels. We investigate the minimum average signal-energy-to-noise ratio required to yield a cutoff rate that is greater than or equal to a given code rate. Also examined are system design issues such as the effect of quantization and metric conversion, the choice between binary codes and M-ary symbol codes, the optimization of the diversity order and the signal size, and the order of deinterleaving and diversity combining. Numerical examples are given to answer concerns raised by these issues.**

I. INTRODUCTION

RECENT years have witnessed a dramatic increase in the demand for cellular radio and paging services in many parts of the world. Terrestrial mobile radio systems, however, are limited in range by tower heights and propagation effects. Furthermore, subscriber costs are dictated by the local population density. In contrast, satellites are ideal for serving nonstationary users over a wide area and can provide costs that are distance insensitive. Many mobile satellite systems have been proposed [1]–[2] and some of them are now in use [2].

Propagation experiments [3]–[7], [24] have indicated that mobile satellite channels suffer from multipath fading and shadowing effects. Diversity and coding techniques are known to be effective measures for mitigating multipath fading [9]–[13], [22]. Although the diversity techniques, when regarded as a special class of coding (repetition codes), do not have respectable transmission efficiency in terms of code rate, they are relative simple to implement and sometimes are the easiest way to remove the residual errors caused by the fading channel's nonzero memory. Differential coherent or noncoherent signaling is an attractive alternative when phase coherency is difficult to attain, such as in cases with multipath fading environments. Uncoded DPSK signaling through a mobile satellite channel was studied by Cygan [8]. M-ary frequency shift keying (MFSK) with various diversity techniques over a Rician or Rayleigh fading channel has been analyzed by Lindsey [9] and Jones [10], among others. The employment of M-ary symbol codes in conjunction with an MFSK signal over fading and/or jammed channels was discussed by Lee [12], Ma [13], Stark [11], [14], and Stüber *et al.* [15]. However, most codes used in practice are binary codes and thus an M-ary-to-binary metric converter is needed [16]. The effect of such a converter on the system performance must be taken into account in designing an MFSK mobile satellite service (MSS). Another practical issue recently raised by McGree and Deaett [17] is the order of deinterleaving and soft-decision combining. They proposed a new predeinterleaving diversity combining technique and showed that the resulting degradation, when compared with the conventional, more sophisticated postdeinterleaving diversity combining, is less than 2 dB in most ranges of interest. A similar issue in the context of mobile satellite environments should also be of interest from a system engineering viewpoint.

When incoherent detection is used in a nonselective slow-fading channel, only the statistic of the received signal envelope or power is of interest in assessing system performance. Propagation models based on experiments have been proposed for mobile satellite channels. Rician distribution has been used in many cases to predict performance in mobile satellite system when a line-of-sight (LOS) path is available [18]. Loo [5] assumed that the LOS signal component under foliage attenuation is lognormal distributed while the multipath component is Rayleigh distributed. Recently, Lutz *et al.* [4], found that their measurements of the MAREC'S mobile satellite signals can best be approximated by a convex combination of a Rician distribution plus a Rayleigh/lognormal distribution. A similar conclusion was reached by Barts and Stutzman [3], [7] who model the shadowed signal as having a Rician/lognormal distribution.

The main purpose of this paper is to investigate the cutoff rate behavior of multichannel MFSK and DPSK signals in four mobile satellite channels mentioned above. Both binary codes and M-ary symbol codes are considered. Comparisons of the predeinterleaving and postdeinterleaving techniques are made and the effect of quantization is investigated. The next section describes the system structure, outlines the basic analysis approach, and presents four mathematical models of the mobile satellite channels. The performance of soft decision decoding is analyzed in Section III. Section IV considers the effect of quantization, compares the predeinterleaving and

Manuscript received January 15, 1994; revised September 3, 1994. This work was supported in part by the National Science Council of Taiwan, under Contract NSC 81-0404-E009-538. This paper was presented in part at the 1991 International Symposium on Communications, Tainan, Taiwan.

The authors are with the Department of Communication Engineering, National Chiao Tung University, Hsinchu, 30049 Taiwan.

IEEE Log Number 9407504.

0733-8716/95$04.00 © 1995 IEEE

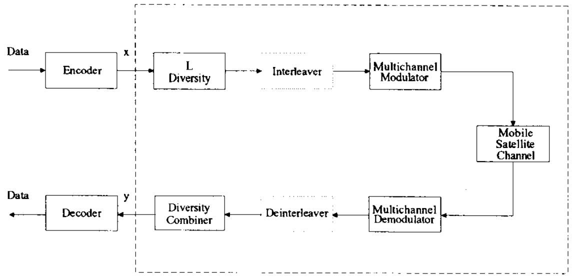

Fig. 1. A coded L-diversity MFSK or DPSK system for mobile satellite communications.

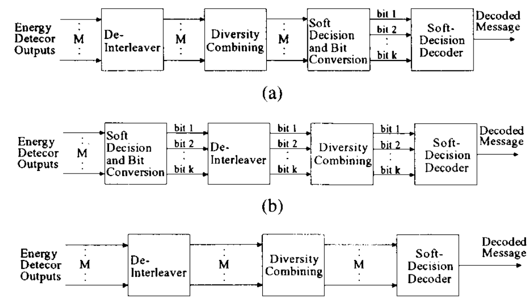

Fig. 2. Three alternatives concerning the order of metric conversion and diversity combining.

postdeinterleaving combinings and analyzes the behavior of M-ary symbol codes.

II. System Description and Channel Models

A. System Architecture

A block diagram of the coded multichannel MFSK communication system is shown in Fig. 1. Each M-ary coded symbol is divided into L subsymbols of equal energy, with each subsymbol transmitted on a different diversity branch. Noncoherent square-law detection is used for each diversity branch. When time diversity is employed, an interleaver at the transmitting end is often used to randomize the sequence of transmitted symbols. A deinterleaver is then needed to unscramble the received signals and to make the *channel* between the interleaver input and the deinterleaver output memoryless. Of course, if other diversity techniques that can ensure independent fading are employed, the interleaver-deinterleaver pair is not needed. The diversity combining scheme considered here is the post-detection equal gain combining scheme. When binary codes are used, a metric conversion algorithm that converts the M-channel demodulator outputs into k numbers is needed.

The three soft decision decoding alternatives to be studied are illustrated in Figs. 2(a)–2(c). For the options shown in Fig. 2(a) (binary code) and Fig. 2(c) (M-ary symbol code), the down-converted data stream is fed into an array of M-bin energy detectors where each detector uses its own in-phase and quadrature phase samples to compute the associated squared magnitudes. Each of these squared magnitudes is fed into a deinterleaver (if needed), which stores the detected bin outputs and then reads them out to the diversity combiner in correct time order. For binary coded systems the incoherently combined detector outputs are then soft-detected using the difference-of-maximums algorithm (see (1) below) to convert the M-ary metric into a k-ary metric, where $k = \log_2 M$. The alternative architecture shown in Fig. 2(b) computes the soft-decision M-bin statistics, converts them into k-bin statistics, and then deinterleaves the soft-detected sequence. The deinterleaver reorders the received bin output sequences and sends them to the diversity combiner. For this option the deinterleaver needs to store only k bins per diversity branch instead of M bins and hence the required memory space is greatly reduced. Let $\{b_i; 1 \le i \le k\}$ be the outputs of the k bins converted from the M-ary outputs of the combiner, $\{a_m; 1 \le m \le M\}$. Then the metric conversion rule under investigation can be expressed as

$$\begin{aligned} b_i &= \text{Max}\{a_m : m \text{ with the } i^{\text{th}} \text{ bit} = \text{“1”}\} \\ &\quad - \text{Max}\{a_m : m \text{ with the } i^{\text{th}} \text{ bit} = \text{“0”}\} \\ &\triangleq b_{i1} - b_{i0}. \end{aligned} \tag{1}$$

Other metric conversion algorithms can be found in [16]. For M-ary codes, the order of deinterleaving and metric conversion is not an issue.

B. Channel Models

Four mobile satellite channels representing different operating scenarios are considered, resulting in four different probability density functions (pdf) for the received signal, as described below. Except for the unshadowed (Rician) model, each model contains at least one parameter that characterizes the long term fading behavior affected by the slowly-changing terrain through which the mobile station moves. We assume that the diversity scheme employed is such that the same parameters can be used to describe the long term fading variations of all diversity branches (see measurement records shown in [4]). In other words, the interleaver-deinterleaver pair in the system has a length long enough to decorrelate the short-term fading but not enough to do so for the long-term fading.

1) Unshadowed, Shadowed, and Mixed Channel of the First Kind: Barts and Stutzman [3], [7] divided received mobile satellite signals into two propagation categories: unshadowed and vegetatively shadowed and proposed a mixed shadowed/unshadowed model. Using a parameter S called the fraction of shadowing they suggested that the overall pdf of the received signal strength be expressed by

$$p_{\text{mix},1}(R) = (1-S)p_{\text{Rice}}(R) + S\int_0^\infty p(R \mid \alpha)p_{\ell n}(\alpha)d\alpha \tag{2}$$

where $p_{\text{Rice}}(R)$ is a Rician pdf and

$$p(R \mid \alpha) = \frac{R}{\sigma^2}\exp\left(-\frac{R^2+\alpha^2}{2\sigma^2}\right)I_0\left(\frac{R\alpha}{\sigma^2}\right), \tag{3}$$

$$p_{\ell n}(\alpha) = \frac{1}{\sqrt{2\pi}d_1\alpha}\exp\left\{-\frac{[\ln(\alpha)-\mu_1]^2}{2d_1^2}\right\} \tag{4}$$

μ_1, d_1 being the mean and standard deviation of $\ln(\alpha)$, respectively. To apply this model to a multichannel system let us consider the special case $S = 0$ first. This is equivalent to the well-known Rician fading channel model. Now define the Rice factor for the nth diversity branch (channel) as $\gamma_n^2 = \alpha_n^2/2\sigma^2$, where α_n is the strength of the LOS component and $2\sigma^2$ represents the mean square value of the multipath component. Clearly, γ^2 is a function of the reflective terrain in the vicinity of the vehicle terminals. Moreover, it is found [7] to be strongly dependent on the elevation angle of the vehicle-satellite line-of-sight.

Using the equal power assumption, $\gamma_n^2 = \gamma^2$, for $n = 1, \cdots, L$, $L =$ the system's diversity order, and the normalization $\alpha_n^2 + 2\sigma^2 = 1$, we can easily show that, when normalized square-law detector outputs from L independent unshadowed channels are combined, the pdf of the resulting sum s is given by

$$p_{\text{Rice}}(s) = \frac{1}{1+\beta}\left(\frac{s}{\Gamma}\right)^{\frac{L-1}{2}} \exp\left(-\frac{s+\Gamma}{1+\beta}\right) I_{L-1}\left(\frac{2\sqrt{s\Gamma}}{1+\beta}\right) \tag{5}$$

where $I_{L-1}(x)$ is the modified Bessel function of order $L-1$,

$$\beta = \frac{1}{1+\gamma^2}\frac{E}{N_0} \triangleq 2\sigma^2\rho$$

$$\Gamma = \sum_{i=1}^{L} \alpha_i^2 \frac{E}{N_0}$$

and $\rho \triangleq (1+\gamma^2)\beta$ is the average signal energy to noise power density ratio per channel.

We next consider another special case, $S = 1$. The resulting distribution is called a shadowed distribution by Loo [5] who assumed that the received signal is composed of a shadowed LOS component and a diffuse component. The former is lognormal distributed while the latter has a Rayleigh distribution with mean square value $2\sigma^2$. The assumption that the direct components of a multichannel signal experience the same shadowing effect implies that $\alpha_i^2 = \alpha^2$ for all $1 \le i \le L$ with probability one. Therefore, the pdf of the normalized combiner output s for this case can also be expressed in a form similar to Loo's shadowed distribution, with $p(R \mid \alpha)$ replaced by

$$p(s \mid \alpha) = \frac{1}{1+\beta}\left(\frac{s}{\alpha^2 L\rho}\right)^{\frac{L-1}{2}} \exp\left(-\frac{s+\alpha^2 L\rho}{1+\beta}\right) \times I_{L-1}\left(2\sqrt{\frac{\alpha^2 sL\rho}{(1+\beta)^2}}\right). \tag{6}$$

Combining both special cases, we then obtain the multichannel version of Barts and Stutzman's model

$$p_{\text{mix},1}(s) = (1-S)p_{\text{Rice}}(s) + S\int_0^\infty p(s \mid \alpha)p_{\ell n}(\alpha)d\alpha. \tag{7}$$

In total, six parameters are needed to characterize such a channel: L, S, μ_1, d_1, γ^2 and the Rice factor for the unshadowed part γ_0^2.

2) Mixed Channel of the Second Kind: From their mobile satellite experiment data, Lutz *et al.* [4] found that the overall received signal power distribution is a convex combination of two different probability density functions governing a 'good' channel state and a 'bad' channel state, respectively. The combination can be characterized by a parameter called the time-share factor A, $0 \le A \le 1$, which is similar to S in the previous mixed model and is a function of the environment and the elevation angle. Therefore, the pdf of the diversity combiner output power s can be expressed as

$$p_{\text{mix},2}(s) = (1-A)p_{\text{Rice}}(s) + A\int_0^\infty p_{\text{Ray}}(s \mid s_0)p_{\log}(s_0)ds_0 \tag{8}$$

where $p_{\text{Rice}}(s)$ is given by (5)

$$p_{\text{Ray}}(s \mid s_0) = \frac{s^{L-1}e^{-s/(1+s_0\rho)}}{(1+s_0\rho)^L(L-1)!} \tag{9}$$

$$p_{\log}(s_0) = \frac{10}{\sqrt{2\pi}d_2 s_0 \ln 10} \times \exp\left\{-\frac{[10\log(s_0)-\mu_2]^2}{2d_2^2}\right\} \tag{10}$$

and μ_2 and d_2 are the mean and standard deviation of $10\log(s_0)$, respectively. The time-varying nature of the shadowing process is reflected on the randomness of the mean received power s_0, which in turn has a lognormal distribution $p_{\log}(s_0)$, as defined in (10). We notice that the second part of this model is different from that of (2) in that, instead of the LOS path, the scattered (Rayleigh faded) component is shadowed.

TABLE I
OPERATING SCENARIOS AND DESIGN ISSUES: TRANSMITTER

Design Issue	Modulation	Coding	Diversity
	DPSK	Binary	Yes (L>1)
Options	MFSK	M-ary	No (L=1)

TABLE II
OPERATING SCENARIOS AND DESIGN ISSUES: COMMUNICATION CHANNEL

Channel	*Parameter*
Rician	Rice factor
Rayleigh	Rice factor = 0
Rayleigh/lognormal	Lognormal: mean, standard deviation
Rician/lognormal	Lognormal: mean, standard deviation
$(1-A)\times$Rician+ $A\times$Rayleigh/lognormal	Rice factor Lognormal: mean, standard deviation

C. System Design Issues

Tables I–III list several important issues concerning the design of a multichannel MFSK or DPSK communication link. We categorize these issues according to the physical subsystem they are associated with, i.e., whether they have to do with the transmitter, the channel, or the receiver. A number of previous related investigations and the operating scenarios they considered are summarized in Table IV. The distinction between our effort and earlier studies can be clearly seen by comparing the tables. Most notably, we consider the combined effect of composite short-term Rician or Rayleigh fading and long-term log-normal fading, the metric conversion (M-ary to binary) loss, the comparison of binary and M-ary codes, and the order of deinterleaving and diversity combining. Some of these issues were discussed in [20] but, as far as we know, none of these issues has been investigated for mobile satellite systems.

TABLE III
OPERATING SCENARIOS AND DESIGN ISSUES: RECEIVER

<table>
<tr><th>Design Issue</th><th>Diversity Combining Scheme</th><th>Metric Conversion</th><th>Order of Deinterleaving and Diversity Combining</th><th colspan="2">Decoding Metric</th></tr>
<tr><td rowspan="3">Options</td><td rowspan="3">Post-detection Equal Gain Combining</td><td>Yes</td><td>Pre-deinterleaving Combining</td><td colspan="2">Hard-decision</td></tr>
<tr><td rowspan="2">No</td><td rowspan="2">Post-deinterleaving Combining</td><td rowspan="2">Soft Decision</td><td>Infinite Precision</td></tr>
<tr><td>Finite Precision</td></tr>
</table>

TABLE IV
SUMMARY OF RELATED INVESTIGATIONS AND THEIR ASSUMPTIONS

Subsystem / *Investigator*	*Modulation*	*Coding*	*Diversity*	*Channel*	*Decoding Metric*
Lindsey [9]	MFSK	no	yes	Rician	*
Lee [12]	8FSK	binary/M-ary	yes	AWGN/jammed	soft
Ma [13]	MFSK	binary/M-ary	yes	AWGN/jammed	soft/hard
Stark [11,14]	MFSK	M-ary	no	Rician, jammed	soft/hard
Stüber [15]	MFSK	M-ary symbol code	yes	Rayleigh/jammed	soft
McGree [17]	MFSK	no	yes	Rayleigh	*
Cygan [8]	DPSK	no	no	composite	*
Su [20]	MFSK	binary/M-ary	yes	AWGN/jammed	soft/hard
Crepeau [23]	MFSK/DPSK	no/binary code	no	Nakagami-m	hard
Rainish [19]	MFSK/MDPSK	M-ary symbol code	no	selective fading	soft

III. CUTOFF RATE PERFORMANCE ANALYSIS

The cutoff rate represents the practical maximum information rate of a coded communication system. The term generalized cutoff rate is sometimes used to emphasize the fact that the metric used by the decoder is not necessarily the maximum log-likelihood metric as the 'conventional' cutoff rate is defined. Maximum likelihood metrics are often too complicated or even impossible (channel statistic is unknown) to implement. If y is the decoder input and x is the encoder output, the decoding metric used in our system is $m(y,x) = yx$, which is the maximum likelihood metric for additive white Gaussian noise channels. For the system shown in Fig. 1, the generalized cutoff rate R_0 (in bits/channel symbol) can be computed via [16]

$$R_0 = 1 - \log_2(1 + D) \tag{11}$$

where

$$D = \min_{\lambda \geq 0} D(\lambda) \tag{12}$$

$$D(\lambda) = E\{e^{\lambda[m(y,x') - m(y,x)]} \mid x \neq x'\} \tag{13}$$

and x, x' are different encoder outputs (1 or -1 in the binary case). The pairwise error bound D is the basis for evaluating decoded BER upper bounds, i.e., in general, $P_b \leq G(D)$ or, equivalently, $P_b \leq B(R_0)$, where $G(\cdot)$ and $B(\cdot)$ are functions determined solely by the specific code used. To evaluate performance for different coding systems, we can first estimate the cutoff rate under a given channel statistic. BER can be obtained subsequently once the associated weight distribution for the code used is known. We shall present performance analysis for MFSK signals only. The performance for incoherent DPSK signaling can be derived from the binary ($M = 2$) case of MFSK system results with a 3 dB shift in required average signal-to-noise ratio.

A. Chernoff Bound for Postdeinterleaving Soft-Decision Decoding

For the binary coded system with postdeinterleaving diversity combining [Fig. 2(a)], we use the soft-decision decoding metric $m(b_i, x) = b_i x$, where b_i is as defined in (1) and $x \in \{+1, -1\}$. This decoding metric is a maximum likelihood metric for AWGN channels.

1) Mixed Channel of the First Kind: For this class of channels, (7) implies that the time intervals corresponding to shadowed and unshadowed regions are disjoint and hence the associated signal strengths follow different and independent probability laws. The resulting Chernoff bound $D_{\text{mix},1}$ is then a convex combination of those obtained under the two separate pdfs, i.e.

$$D_{\text{mix},1} = (1-S)\operatorname*{Min}_{\lambda \geq 0} D_{\text{Rice}}(\lambda) + S\int_0^\infty \left[\operatorname*{Min}_{\lambda \geq 0} D_{\text{Rice/ln}}(\lambda; r)\right] p_{\ell n}(r)\,dr. \tag{14}$$

In the second term of the above expression we have minimized over λ before taking the expectation with respect to r. This is a result of the assumption that r is a function of the receiver's environment which changes very slowly with respect to the data rate and thus the LOS components from each diversity suffer from the same shadowing effect simultaneously. Using a procedure similar to that given in [20] we can show that the nonminimized Chernoff bounds (NCB) $D_{\text{Rice}}(\lambda)$ and $D_{\text{Rice/ln}}(\lambda, r)$ in (14) are given by

$$\begin{aligned} D_{\text{Rice}}(\lambda) &= \left[\frac{M}{2}\sum_{i=0}^{M/2-1}(-)^i\binom{M/2-1}{i}\sum_{k=0}^{i(L-1)}\frac{c_{i,k}(L)_k}{(1+i-\lambda)^{L+k}}\right] \\ &\quad\times\left[\frac{M/2-1}{(L-1)!}\sum_{n=0}^{M/2-2}(-1)^n\binom{M/2-2}{n}\right. \\ &\quad\times\sum_{j=0}^{n(L-1)}c_{n,j}Q(n+1+\lambda, L+j-1) \\ &\quad+\sum_{m=0}^{M/2-1}(-1)^m\binom{M/2-1}{m} \\ &\quad\left.\times\sum_{\ell=0}^{m(L-1)}c_{m,\ell}P(m+\lambda,\ell)\right] \end{aligned} \tag{15}$$

and

$$\begin{aligned} D_{\text{Rice/ln}}(\lambda; r) &= \left[\frac{M}{2}\sum_{i=0}^{M/2-1}(-1)^i\binom{M/2-1}{i}\right. \\ &\quad\left.\times\sum_{k=0}^{i(L-1)}c_{i,k}\frac{(L)_k}{(1+i-\lambda)^{L+k}}\right] \\ &\quad\times\left[\frac{M/2-1}{(L-1)!}\sum_{n=0}^{M/2-2}(-1)^n\binom{M/2-2}{n}\right. \\ &\quad\times\sum_{j=0}^{n(L-1)}c_{n,j}Q(n+1+\lambda, L+j-1; r) \\ &\quad+\sum_{\ell=0}^{M/2-1}(-1)^\ell\binom{M/2-1}{\ell} \\ &\quad\left.\times\sum_{k=0}^{\ell(L-1)}c_{\ell,k}P(\ell+\lambda, k; r)\right] \end{aligned} \tag{16}$$

where $(L)_k = (L+k-1)!/(L-1)!$, $c_{n,k}$[1] is the coefficient of x^k in the expansion

$$\left(\sum_{i=0}^{L-1} \frac{x^i}{i!}\right)^n = \sum_{k=0}^{n(L-1)} c_{n,k} x^k \tag{17}$$

and

$$P(\lambda,k) = \left[\frac{1}{1+\lambda(1+\beta)}\right]^L \exp\left[\frac{-\lambda\Gamma}{1+\lambda(1+\beta)}\right] \cdot (L)_k \times \left[\frac{1+\beta}{1+\lambda(1+\beta)}\right]^k \times {}_1F_1\left(-k, L; \frac{-\Gamma}{(1+\beta)(1+\lambda(1+\beta))}\right). \tag{18}$$

$Q(\lambda,k)$ is related to $P(\lambda,k)$ via

$$Q(\lambda,k) = \frac{kQ(\lambda,k-1)+P(\lambda,k)}{\lambda} \tag{19}$$

${}_1F_1(a,b;z)$ is the confluent hypergeometric function, $P(\lambda,k;r)$ and $Q(\lambda,k;r)$ are derived from $P(\lambda,k)$ and $Q(\lambda,k)$ (see (18), (19)) with the substitution $\Gamma = r^2 L\rho$. The Chernoff bound for an unshadowed (Rician) or shadowed (Rician/lognormal) channel alone can be obtained by setting $S=0$ or $S=1$ in the related equations. If binary FSK is employed in a Rician channel, direct substitution of $M=2$ into (15) and (18) leads to

$$D_{\mathrm{Rice}}(\lambda) = \frac{1}{(1-\lambda)^L} P(\lambda,0). \tag{20}$$

2) Mixed Channel of the Second Kind: Similar to the previous case, the 'good' channel states and 'bad' channel states in mixed channel of the second kind are disjoint and the corresponding Chernoff bound can be shown to be

$$D_{\mathrm{mix},2} = (1-A) \underset{\lambda\ge 0}{\mathrm{Min}}\, D_{\mathrm{Rice}}(\lambda) + A \int_0^\infty \left[\underset{\lambda\ge 0}{\mathrm{Min}}\, D_{\mathrm{Ray/log}}(\lambda; s_0)\right] p_{\log}(s_0)\, ds_0 \tag{21}$$

where $D_{\mathrm{Rice}}(\lambda)$ is defined by (15) and

$$D_{\mathrm{Ray/log}}(\lambda;s_0) = \left[\frac{M}{2}\sum_{i=0}^{M/2-1}(-1)^i\binom{M/2-1}{i}\sum_{k=0}^{i(L-1)} c_{i,k}\frac{(L)_k}{(1+i-\lambda)^{L+k}}\right] \times \left[\frac{M/2-1}{(L-1)!}\sum_{m=0}^{M/2-2}(-1)^m\binom{M/2-2}{m} \times \sum_{k=0}^{m(L-1)} c_{m,k}\, q(m+1+\lambda, L+k-1; s_0) + \sum_{n=0}^{M/2-1}(-1)^n\binom{M/2-1}{n}\sum_{k=0}^{n(L-1)} c_{n,k}\, p(n+\lambda,k;s_0)\right] \tag{22}$$

[1] We have omitted the dependence of the coefficient $c_{n,k}$ and some other functions on L because throughout our discussion the degree of the polynomial on the right side of (17) is always $L-1$.

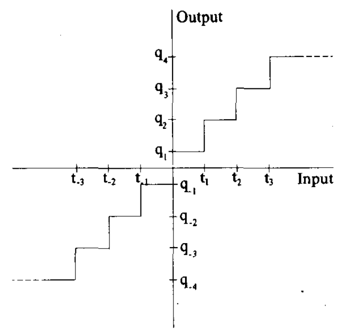

Fig. 3. A Q steps midrise uniform quantizer ($Q = 8$).

and

$$p(\lambda,k;s_0) = (L)_k (1+s_0\rho)^k \left(\frac{1}{1+\lambda+\lambda s_0\rho}\right)^{L+k}. \tag{23}$$

$p(\lambda,k;s_0)$ and $q(\lambda,k;s_0)$ are related by an equation similar to (19).

IV. Quantization, Predeinterleaving and M-ary Codes

We now present analysis pertaining to the three practical design issues raised in Section II(c). Quantization is an important concern because no infinite precision arithmetic can be implemented in digital domain. Predeinterleaving diversity combining can save memory space, as demonstrated in [17]. It is worthwhile to see how much degradation we have to pay for a certain amount of hardware savings. The cutoff rate performance of M-ary symbol codes can be used to predict their coded BER and to compare it with that of binary codes.

A. Effects of Quantization and Predeinterleaving Combining

For the midrise N-level ($N = 2^k$ for some integer k) quantizer shown in Fig. 3. The probability distributions at the quantizer output can be derived from the well-known inversion formula or an alternative form by Gil-Palaez (pp. 153–159, [25]) that relate them to the characteristic functions of the input. If we define $\epsilon_{-N/2} = \Pr(-\infty < y < t_{-N/2+1})$, $\epsilon_i = \Pr(t_i < y \le t_{i+1})$, and $\epsilon_{N/2} = \Pr(t_{N/2} < y < \infty)$, where $\{t_i, i = 0, \pm 1, \cdots, \pm(\frac{N}{2}-1)\}$ are the quantizer thresholds, y is a random variable representing the quantizer's input then the corresponding NCB can be written as

$$D(\lambda) = \sum_{n=1}^{\frac{N}{2}} [\epsilon_n e^{\lambda(2n-1)} + \epsilon_{-n} e^{-\lambda(2n-1)}]. \tag{24}$$

The cutoff rate of the predeinterleaving soft decision decoding system [Fig. 2(b)] can be computed by appropriate modification of R_0 expression for the post-deinterleaving system. Since the statistics for the outputs from various diversity channels are assumed to be independent, the corresponding nonminimized Chernoff bound $D'(\lambda)$ can be calculated via

$$D'(\lambda) = \left[D(\lambda)\mid_{L=1,\beta=2\sigma_0^2 E/N_0}\right]^L \tag{25}$$

where $D(\lambda)$ is given by (14), (15), or (21). Note that both predeinterleaving and post-deinterleaving decoding metrics yield the same statistics when $L = 1$ or $M = 2$. On the basis of the above equation and our earlier results on the post-deinterleaving diversity combining receivers, cutoff rate performance in various mobile satellite channels can be evaluated.

B. M-ary Symbol Code Performance

If an M-ary symbol code is employed in conjunction with the MFSK signals and we use the energy metric $m(A, n) = a_n$ [16], where $\{a_n\}$, $n = 1, \cdots, M$, are the M-ary outputs from the diversity combiner, then it can be shown that the Chernoff bound for the Rician channel is

$$D_{\text{Rice},M} = \operatorname*{Min}_{\lambda \geq 0} \frac{\exp\left[\frac{-\lambda\Gamma}{1+(1+\beta)\lambda}\right]}{[(1-\lambda)(1+(1+\beta)\lambda)]^L} = \frac{\exp\left[\frac{-\lambda_{\text{Rice}}\Gamma}{1+(1+\beta)\lambda_{\text{Rice}}}\right]}{[(1-\lambda_{\text{Rice}})(1+(1+\beta)\lambda_{\text{Rice}})]^L} \qquad (26)$$

where [see (27) below]. The Chernoff bound for Loo's shadowed channel is

$$D_{\text{Rice/ln,M}} = \int_0^\infty \left\{ \operatorname*{Min}_{\lambda \geq 0} \frac{\exp\left[\frac{-\rho L \lambda r^2}{1+(1+\beta)\lambda}\right]}{(1-\lambda)^L[1+(1+\beta)\lambda]^L} \right\} p_{\ell n}(r)dr = \int_0^\infty \left\{ \frac{\exp\left[\frac{-\rho L \lambda_{\text{Rice/ln}} r^2}{1+(1+\beta)\lambda_{\text{Rice/ln}}}\right]}{(1-\lambda_{\text{Rice/ln}})^L[1+(1+\beta)\lambda_{\text{Rice/ln}}]^L} \right\} \times p_{\ell n}(r)dr \qquad (28)$$

where [see (29) below], while that for the Rayleigh channel is

$$D_{\text{Ray/log},M} = \int_0^\infty \left\{ \operatorname*{Min}_{\lambda \geq 0} \frac{1}{(1-\lambda)^L[1+(1+s_0\rho)\lambda]^L} \right\} p_{\log}(s_0)ds_0 = \int_0^\infty \frac{(1+s_0\rho)^L}{(1+s_0\rho/2)^{2L}} p_{\log}(s_0)ds_0. \qquad (30)$$

The Chernoff bound D for a mixed channel can be readily obtained from appropriate combination of the above bounds. The resulting cutoff rate R_0, when measured in information symbols per code symbol (for binary codes, an information symbol is equal to an information bit), is [16]

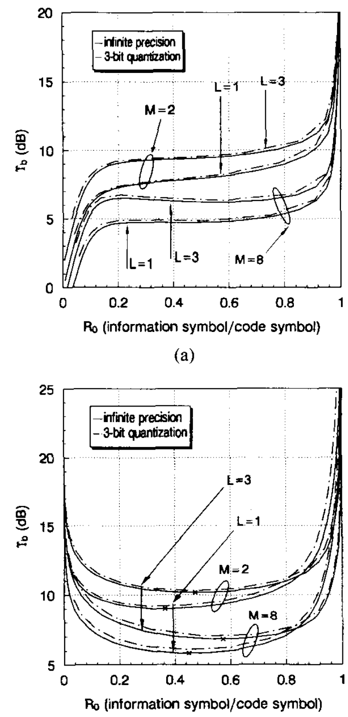

Fig. 4. Effects of diversity order (L), modulation complexity (M) and quantization on the coded performance of MFSK signaling in (a) a mixed channel of the first kind, (b) a mixed channel of the second kind; optimal code rates are marked by ×.

$$R_0 = 1 - \log_M [1 + (M-1)D]. \qquad (31)$$

V. Numerical Results and Discussion

Numerical behavior of cutoff rate is often evaluated as a function of channel symbol energy to noise power level ratio $\Upsilon_{cs} \stackrel{\text{def}}{=} \rho(L/\log_2 M)$ [19]. But if we consider a fixed signal energy per information bit scenario, it would be more insightful to present R_0 as a function of the ratio of the average information bit energy and the noise power level, $\Upsilon_b = \Upsilon_{cs}/(r \log_2 M) = \rho(L/r \log_2 M)$ [11, 14, 15], assuming a rate $r = R_0$ code is used. Since $R_0 = f(\Upsilon_{cs})$, where $f(\cdot)$ is a highly nonlinear function, to have reliable and implementable

$$\lambda_{\text{Rice}} = \frac{-\Gamma - (2+\beta-\beta^2)L + \sqrt{8L(\Gamma+\beta L)(1+\beta)^2 + (\Gamma + 2L + \beta L - \beta^2 L)^2}}{4L(1+\beta)^2} \qquad (27)$$

$$\lambda_{\text{Rice/ln}} = \frac{\beta^2 - \beta - \rho\gamma^2 - 2 + \sqrt{4 + 12\rho\gamma^2 + \rho^2\gamma^4 + 6(2+3\rho\gamma^2)\beta + (13+6\rho\gamma^2)\beta^2 + 6\beta^3 + \beta^4}}{4(1+\beta)^2} \qquad (29)$$

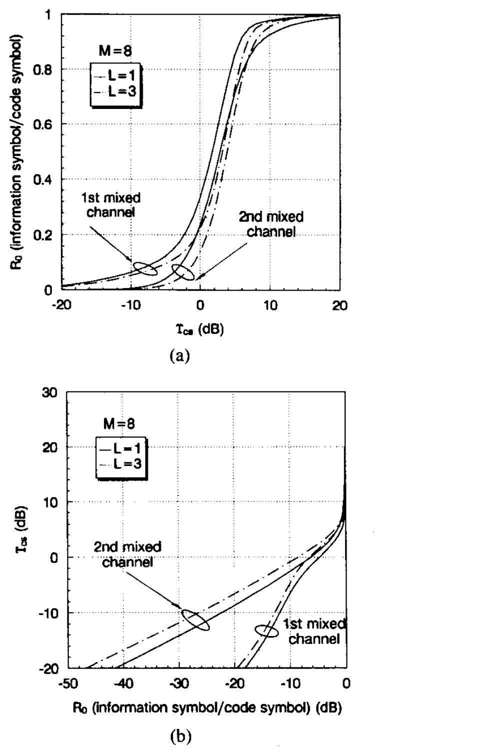

Fig. 5. Cutoff rate performance of MFSK signaling in mixed channels: (a) R_0 (linear scale) versus Υ_{cs} (b) Υ_{cs} versus R_0 (dB).

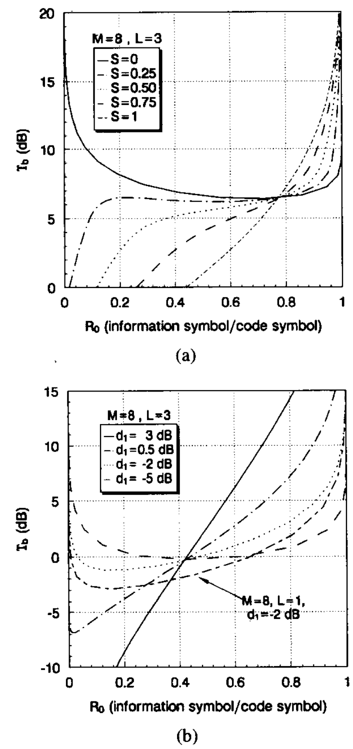

Fig. 6. (a) Effect of the fraction of shadowing on the coded performance of MFSK signaling in a mixed channel of the first kind; $S = 0$ represents the case of a pure Rician fading channel. (b) Effect of the degree of shadowing on the coded performance of MFSK signaling in a Rician/lognormal channel.

communication at a code rate $r = R_0$ we must have

$$\Upsilon_b \geq \frac{f^{-1}(r)/r}{\log_2 M} \stackrel{\text{def}}{=} \frac{g(r)}{\log_2 M}. \quad (32)$$

In other words, if we interpret R_0 in the following figures as the code rates r used then the values in the corresponding vertical axes give the minimum Υ_b needed for $R_0 \geq r$.

Figs. 4(a)–5(b) depict coded performance for two mixed channels. Figs. 5(a)–5(b) are included to illustrate the relationship between $R_0 = f(\Upsilon_{cs})$ and $\Upsilon_b = f^{-1}(R_0)/(R_0 \log_2 M)$. The parameters for the mixed channel of the first kind are: $S = .25$, $d_1 = .5$ dB, $\mu_1 = -1$ dB, $\gamma^2 = 18$ dB, $\gamma_0^2 = 22$ dB and those for the second mixed channels are: $A = .25$, $d_2 = 6$ dB, $\mu_2 = -7.7$ dB and the Rice factor for the pure Rician part is 11.9 dB. It is clear that R_0 is an increasing function of the modulation complexity M within the range of interest and 3-bit quantization incurs only negligible loss (<.2 dB in most cases). Coding is most effective in combating multipath fading when the code rate is not too high so that enough encoding redundancy is available. However, the usefulness of coding is greatly reduced or even diminishes if the signal does not have enough power to overcome thermal noise in the first place; see Fig. 5(a). For the first mixed model, the increase of L results in performance degradation for almost all but those R_0 that are very close to one (for the cases shown here R_0 must be greater than .9989). This is a drastic departure from the conventional prediction that suitable increase of diversity order can enhance the system performance in a fading channel. On the other hand, in a mixed channel of the second kind, the increase of the diversity order does improve the performance when the code rate is high (> .8).

Define the optimal code rate as the one for which the required Υ_b to achieve reliable communication is minimized. Then we note that optimal code rates exist for the second mixed channel but not the first one. (32) implies that a local minimum Υ_b is achieved by using the optimal code rate r_{opt} which satisfies the condition

$$\left.\frac{dg(r)}{dr}\right|_{r=r_{\text{opt}}} = 0, \quad \left.\frac{d^2g(r)}{d^2r}\right|_{r=r_{\text{opt}}} > 0 \quad (33)$$

which can be shown to be equivalent to

$$\left.\frac{d\ln[g(r)]}{d\ln(r)}\right|_{r=r_{\text{opt}}} = 1 \quad (34a)$$

$$\left.\frac{d^2\ln[g(r)]}{d^2\ln(r)}\right|_{r=r_{\text{opt}}} > 0. \quad (34b)$$

Comparisons of Figs. 4(b)–5(b) reveal that, though local minimums exist for both mixed channels, there is no global minimum (at least within the range of interest) for the first

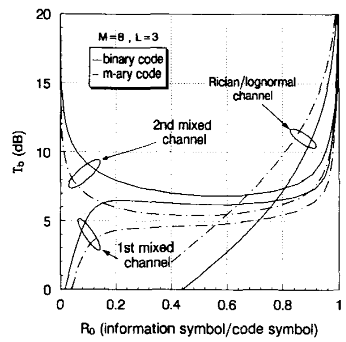

Fig. 7. Comparison of binary and M-ary symbol coded performance of MFSK signaling in various mobile satellite channels.

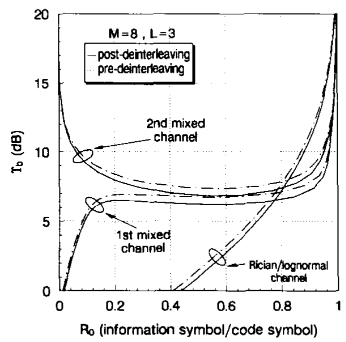

Fig. 8. Coded performance of the post-deinterleaving and predeinterleaving diversity combining schemes for MFSK signals in various mobile satellite channels.

mixed channel. This is because the latter channel [Fig. 5(b)] does not satisfy the convexity requirement (34b). More examples of the coded behavior under the first mixed channel are provided in Figs. 6(a)–6(b). These curves indicate that the nonexistence of an optimal code rate is due to the fact that all diversity branches suffer from the same long-term (or large-area) fading. This fact also explains why the increase of the diversity order does not always lead to performance improvement for the first mixed model. Further examinations of the cases 1) $S = 0$ [Fig. 6(a)] and 2) $S = 1$ with small d_1 [Fig. 6(b)] tell us that an optimal code rate exists if there is Rician fading only or if the Rician/lognormal fading is not significant (small deviations). We observe that Rician channels are less sensitive to the choice of the code rate and, for the mixed channel of the first kind, the sensitivity is an increasing function of d_1 but a decreasing function of S at the high code rate region. However, we want to emphasize that the cases $d_1 < 0$ dB are not typical [24].

Fig. 7 offers comparison of binary codes and M-ary symbol codes for various channels. The two mixed channels are the same channels used in Figs. 4(a)–6(b) and the Rician/lognormal channel has the same set of parameters as those of the shadowed part of the first mixed channel. It is found that, for both classes of mixed channels, the M-ary to binary conversion results in a 1∼2.1 dB loss. However, M-ary symbol codes are not always better than binary codes, e.g., the latter have a 2∼2.7 dB advantage in pure Rician/lognormal channels. This is because the decoding metric for both classes of codes are not ML metrics. Finally, Fig. 8 gives comparison between the predeinterleaving and the post-deinterleaving diversity combining schemes. The degradation resulting from using the simpler predeinterleaving combining is not significant (<1 dB for almost all cases). This result is similar to the conclusion obtained in [17] and [20].

REFERENCES

[1] J. D. Kiesling, "Land mobile satellite systems," in *Proc. IEEE*, pp. 1107–1115, July 1990.

[2] "Second International Mobile Satellite Conference (IMSC)," in *Session 1, Proc. IMSC '90* (Ottawa, Canada), June 1990, pp. 3–36.

[3] R. M. Barts and W. L. Stutzman, "Propagation modeling for land mobile satellite systems," in *Proc. IMSC'88, 1st Int. Mobile Satellite Conf.*, May 1988, pp. 95–100.

[4] E. Lutz *et al.*, "The land mobile satellite communication channels-recording, statistics and channel model," *IEEE Trans. Veh. Technol.*, vol. 40, no. 2, pp. 375–385, May 1991.

[5] C. Loo, "A statistical model for a land mobile satellite link," *IEEE Trans. Veh. Technol.*, vol. VT-34, no. 3, pp. 122–127, Aug. 1985.

[6] D. Cygan, M. Dippold, and J. Finkenzeller, "Models for the land mobile satellite channel," *Archiv. Elec. Ubertr.*, vol. 42, pp. 329–339, Nov/Dec. 1988.

[7] R. M. Barts and W. L. Stutzman, "Modeling and simulation of mobile satellite propagation," *IEEE Trans. Antenn. Propagat.*, vol. 40, pp. 375–382, Apr. 1992.

[8] D. Cygan, "Analytical evaluation of average bit error rate for the land mobile satellite channel," *Int. J. Sat. Commun.*, vol. 7, no. 2, pp. 99–102, Apr.–June 1989.

[9] W. C. Lindsey, "Error probabilities for Rician fading multichannel reception of binary and N-ary signals," *IEEE Trans. Inform. Theory*, vol. IT-10, pp. 339–350, Oct. 1964.

[10] J. J. Jones, "Multichannel FSK and DPSK reception with three-component multipath," *IEEE Trans. Commun.*, vol. COM-16, pp. 808–821, Dec. 1966.

[11] W. E. Stark, "Coding for frequency-hopped spread-spectrum communication with partial-band interference—Part I: Capacity and cutoff rate," *IEEE Trans. Commun.*, vol. COM-33, pp. 1036–1044, Oct. 1985.

[12] J. S. Lee, L. E. Miller, and R. H. French, "Error-correcting codes and nonlinear diversity combining against worst case partial-band noise jamming of frequency-hopping MFSK systems," *IEEE Trans. Commun.* vol. 36, pp. 471–478, Apr. 1988.

[13] H. H. Ma and M. A. Poole, "Error-correcting codes against the worst-case partial band jammer," *IEEE Trans. Commun.* vol. COM-32, no. 2, pp. 124–133, Feb. 1984.

[14] W. E. Stark, "Capacity and cutoff rate of noncoherent FSK with nonselective Rician fading," *IEEE Trans. Commun.*, vol. COM-33, pp. 1153–1159, Nov. 1985.

[15] G. L. Stüber, J. W. Mark, and I. F. Blake, "Diversity and coding for FH/MFSK systems with fading and jammer—Part I: Multichannel diversity," *IEEE Trans. Commun.*, vol. COM-35, pp. 1329–1340, Dec. 1987.

[16] M. K. Simon *et al.*, *Spread Spectrum Communications*, vol. I. Rockville, MD: Computer Science Press, 1985.

[17] T. McGree and M. Deaett, "Predeinterleaving soft decision performance for MFSK detection on the Rayleigh fading channels," in *Conf. Rec., MILCOM '89*, Oct. 1989, pp. 39.2.1–39.2.7.

[18] M. K. Simon and D. Divsalar, "The performance of trellis coded multilevel DPSK on a fading mobile satellite channel," *IEEE Trans. Veh. Technol.*, vol. 37, no. 2, pp. 78–91, May 1988.

[19] D. Rainish and J. M. Perl, "Generalized cutoff rate of time- and frequency-selective fading channels," *IEEE Trans. Commun.*, vol. 37, pp. 449–467, May 1989.

[20] Y. T. Su and R. C. Chang, "Performance of fast FH/MFSK signals in jammed binary channels," *IEEE Trans. Commun.*, vol. 42, no. 7, pp. 2414–2422, Jul. 1994.

[21] D. T. Lai, "A study on mobile satellite service with multichannel MFSK and DPSK signals," M.S. thesis, Chiao Tung University, June 1992.

[22] J. G. Proakis, *Digital Communications*, 2nd ed. New York: McGraw-Hill, 1989, ch. 8

[23] P. J. Crepeau, "Uncoded and coded performance of MFSK and DPSK in Nakagami fading channels," *IEEE Trans Commun.*, vol. 40, no. 3, pp. 487–494, Mar. 1992.
[24] J. Goldhirsh and W. J. Volgel, "Propagation effects for land mobile satellite systems: overview of experimental and modeling results," *NASA Ref. Publicat. 1274*, 1992.
[25] K. L. Chung, *A Course in Probability Theory.* New York: Academic, 1974, ch. 6.

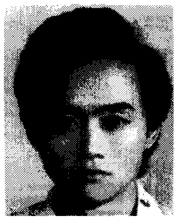

Yu T. Su (S'81–M'83), received the B.S.E.E. degree from Tatung Institute of Technology, Taiwan in 1974, and the M.S. and Ph.D. degrees from the University of Southern California in 1983.

From May 1983 to September 1989, he was with LinCom Corporation, Los Angeles. He is currently a faculty member in the Department of Communications Engineering and the Microelectronic and Information System Research Center for the National Chiao Tung University. His present research interests are in the areas of communication theory and statistical signal processing.

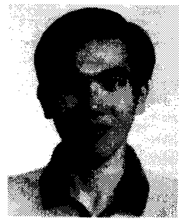

Ju-Ya Chen was born in Kaohsiung, Taiwan, on April 5, 1970. He received the B.S. and M.S. degrees in communication engineering from the National Chiao Tung University, Hsinchu, Taiwan, in 1992 and 1994, respectively. He is currently working toward the Ph.D. degree at the same university.

His research interests include detection, estimation, and spread spectrum communication systems.